Article

Journal of the Brazilian Chemical Society

https://dx.doi.org/10.21577/0103-5053.20250010

J. Braz. Chem. Soc. **2025**, *36*, 5, e-20250010, 1-9

A Spectrophotometric Study of the Interaction of Quercetin and Tannic Acid with Mimetic Systems of Cancerous and Healthy Cells

Pablo A. Oliveira,[a] Leandro A. Mendes,[a] Vitor O. Silva,[a] Paulo V. Scarparo,[a] Layra C. Conceição,[a] Pedro I. S. Maia,[a] Jéferson A. Moreto[b] and Natália B. L. Slade[*,a]

[a]Instituto de Ciências Exatas, Naturais e Educação, Universidade Federal do Triângulo Mineiro, 38064-200 Uberaba-MG, Brazil

[b]Departamento de Engenharia de Materiais, Escola de Engenharia de São Carlos, Universidade de São Paulo, 13566-590 São Carlos-SP, Brazil

Quercetin (QUE) and tannic acid (TA) are among the antioxidants that have been shown efficiency in the treatment and prevention of cancer, cardiovascular and neurodegenerative diseases. However, little is known about the mechanisms by which these activities occur. Hereupon, this work presents a spectrophotometric study on their interaction with mimetic systems of cancerous and healthy cells. The objective was to evaluate the relevance of changes in pH and lipid composition of cell membranes, triggered by cancer development, in the target-antioxidant interaction. Therefore, intrinsic spectrophotometric properties of these compounds were monitored under different conditions. Results showed that QUE and TA were able to partition significantly from the aqueous medium to the model membranes. However, the partitioning was shown to be dependent on the lipid composition and pH. Partition coefficients, partition free energy, spectral shifts and turbidity parameters were also obtained, indicating that there is a balance between electrostatic and non-electrostatic interactions in the system that depends on the hydrophobicity/hydrophilicity of the polyphenols and the number of groups available for hydrogen bonding. In fact, this reveals that lipid composition and pH of the cellular microenvironment play an important role in their activity, influencing their ability to differentiate between healthy from cancer cells.

Keywords: antioxidants, interaction mechanisms, lipid mimetic membranes, asymmetric model membranes, asymmetric large unilamellar vesicles, spectrophotometric analysis

Introduction

Cancer affects millions of individuals globally, and its treatment options are often accompanied by numerous side effects and potential risks to patients. Consequently, there is a pressing need to explore new therapeutic approaches and medications.[1-5] Natural antioxidants present a promising alternative as they tend to be less invasive and toxic, while demonstrating efficacy in the prevention and treatment of cancer, as well as cardiovascular and neurodegenerative diseases.[6]

Quercetin (QUE) and tannic acid (TA) are part of this class of bioactive compounds, and extensive research has been conducted on their anticancer properties.[7-13] Their chemical structure is represented in Figure 1. The current literature[1-5,10-17] highlights an extensive search for alternatives to harness these biomolecules as therapeutic agents or in complementary strategies. Among these, nanotechnology has emerged as a pivotal approach, significantly enhancing the bioavailability and absorption efficiency of these bioactives. Despite their potential, the mechanisms of action of these compounds remain poorly understood, primarily due to their broad range of interactions with various receptors and enzymes. Given that many of these interactions occur at the cell membrane level, studying the interaction between antioxidants and the lipid bilayer becomes crucial.[18] Such investigations provide valuable insights into the distribution parameters of these compounds within the microenvironment, enabling the establishment of relationships between their physicochemical properties and their mechanisms of action. This knowledge is essential for advancing their therapeutic potential and optimizing their application.

*e-mail: natalia.slade@uftm.edu.br
Editor handled this article: Fernando C. Giacomelli (Associate)

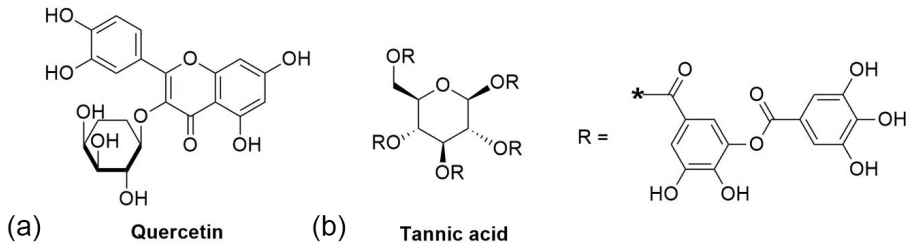

Figure 1. Chemical structures of (a) quercetin and (b) tannic acid.

In this context, the objective of the present study was to offer an initial insight into the interactions of the antioxidants QUE and TA with mimetic cell membrane systems. Our focus was to assess how alterations triggered by cancer may affect the interaction of these antioxidants with the lipid bilayer, in a controlled and simplified environment. For this purpose, it was performed a spectrophotometric study of QUE and TA interactions with large unilamellar vesicles (LUVs) that mimic the membranes of healthy and cancer cells. The characteristic pHs of the cellular microenvironments of interest were considered, as well as the specific lipid compositions of each system. The healthy microenvironment has a physiological pH around 7.4 and the lipid composition is abundant in phosphatidylcholine (PC) and sterol cholesterol.[19] The cancerous microenvironment has an acidic pH ca. 5.5, due to the high production of lactic acid given the high rate of cell reproduction triggered by the development of the disease.[20] In addition, the lipid composition of this system involves the presence of phospholipids: PC, phosphatidylethanolamine (PE) and phosphatidylserine (PS), as well as the sterol cholesterol.[21] This variation is also consequence of the cancer development, in which the lipid asymmetry of healthy cells is disrupted causing phospholipids abundant in the inner monolayer to be exteriorized in the outer monolayer.[21] The antioxidants interaction under the aforementioned conditions was evaluated by UV-Vis spectroscopy, making it possible to investigate both their spectroscopic properties in the environments of interest as well as their affinity for the model systems.

Experimental

Chemicals

Phospholipids and cholesterol (Chol) were obtained from Avanti Polar Lipids®: 1-palmitoyl-2-oleoyl-*sn*-glycero-3-phosphocholine (PC), 1-palmitoyl-2-oleoyl-*sn*-glycero-3-phosphatidylethanolamine (PE) and 1-palmitoyl-2-oleoyl-*sn*-glycero-3-phosphatidylserine (PS). QUE and TA were supplied by Sigma-Aldrich Co. (St. Louis, USA). Other chemicals were of high-quality analytical or spectroscopic grade.

Antioxidant solutions and buffer preparation

For partition coefficient determination, QUE and TA solutions were prepared by diluting 2 mg in 1.5 mL of 0.6% (v/v) dimethyl sulfoxide (DMSO). The experiments were carried out at pHs 5.5 and 7.4 with a buffer solution composed of 0.15 mol L^{-1} citrate-phosphate and 150 mmol L^{-1} NaCl.

Preparation of large unilamellar vesicles (LUVs)

Lipid stock solutions were mixed in chloroform to give the following compositions: PC/Chol (80:20) and PC/PE/PS/Chol (30:25:25:20), at the approximate concentration of 3 mmol L^{-1}. Lipid mixtures were submitted to evaporation of the solvent under N_2 flow followed by drying under vacuum over 3 h. The films were hydrated by the addition of a 0.15 mol L^{-1} citrate-phosphate buffer containing 150 mmol L^{-1} NaCl, pH 7.4 and pH 5.5. These suspensions were homogenized by vortexing for 2.5 min. To obtain the LUVs, after homogenization, the suspension was subjected to extrusion through polycarbonate membranes (6 and 11-times in 400 and 100 nm pore size membranes, respectively) in an Avanti mini extruder. LUVs were kept under refrigeration, protected from light, and used within 24 h of preparation. LUVs average hydrodynamic diameters were accessed by using a Zetasizer (Malvern Instruments, Worcestershire, UK), presenting values around 140 nm.

Preparation of asymmetric large unilamellar vesicles (aLUVs)

The preparation of aLUVs was based on Doktorova *et al.*[22] in which two distinct thin films of phospholipids were prepared in the desired composition for each leaflet of the asymmetric model membrane. The acceptor vesicles compose the inner monolayer, made of PE/Chol (80:20), while the donor vesicles compose the outer leaflet, made of PC/Chol (80:20). The lipids were diluted with chloroform

in round-bottom glass tubes. The solvent was evaporated under a stream of N_2 and completely dried under vacuum for at least three hours. Subsequently, the films were hydrated by adding the citrate/phosphate buffer containing 150 mmol L^{-1} NaCl, at pH 7.4, at 45 °C, then the suspension was homogenized by vortexing for three minutes. To obtain the acceptor vesicles, the suspension was extruded through polycarbonate membranes (six times through 400 nm membranes and 11 times through 100 nm membranes) using an Avanti mini-extruder. For the donor vesicles, lipid film was hydrated with a 300 mmol L^{-1} sucrose solution to reach a final concentration of 20 mg mL^{-1} at 50 °C. The suspension was diluted in Milli-Q water and centrifuged for 30 min at 20,000 g, at 20 °C. The supernatant was discarded, and the pellet was resuspended in a 35 mmol L^{-1} methyl-beta-cyclodextrin (mβCD) solution to achieve an 8:1 mβCD:lipid ratio. The donor suspension was incubated under magnetic stirring for 2 h at room temperature. Subsequently, the acceptor and donor vesicle suspensions were mixed and incubated for an additional 30 min under moderate stirring at 250 rpm. Finally, they were purified by centrifugation using a 100 kDa centrifugal filter device. aLUVs average hydrodynamic diameters were accessed by using a Zetasizer (Malvern Instruments, Worcestershire, UK), presenting values around 160 nm.

Spectrophotometric titration

Spectrophotometric titrations were performed in three formats: (*i*) determination of the molar absorptivity coefficient (ε) of antioxidants in buffer solution at pHs 5.5 and 7.4; (*ii*) antioxidants ε determination in the presence of cancer cells and healthy model membranes (PC/PE/PS/Chol at pH 5.5 and PC/Chol at pH 7.4, respectively); and (*iii*) determination of partition coefficients (K_P) of antioxidants by the systems of interest and the associated spectral shifts.

Increasing concentrations of quercetin (0 to 60 μmol L^{-1}) and tannic acid (0 to 85 μmol L^{-1}) were used to investigate their intrinsic absorbance as a function of concentration in the absence and presence of 100 μmol L^{-1} of LUVs. The respective spectra were recorded from 250 to 500 nm with a UV-Vis spectrophotometer Shimadzu UV 2600 model (Shimadzu Corp Japan). The maximum absorbances of each concentration were used to construct the graph, which after linear adjustment provides the ε.

To determine K_P, the antioxidants at 20 μmol L^{-1} were titrated with the LUVs suspension from 0 to 2 mmol L^{-1}. The absorption spectra were also recorded from 250 to 500 nm. The second derivative was obtained to determine the wavelength of maximum absorbance.[23] The maximum absorptions were recorded afterwards and plotted in a graph as a function of the lipid concentration, for the construction of the isotherm partitions. K_P values were obtained by fitting plots with the equation below:

$$\frac{Abs(L)}{Abs_0} = 1 + \left(\frac{Abs_{max}}{Abs_0} - 1 \right) \times \frac{K_P \gamma_L [L]}{1 + K_P \gamma_L [L]} \quad (1)$$

where Abs(L), Abs_0 and Abs_{max} are, respectively, the absorbance in the presence of LUVs, in the absence, and the maximum absorbance obtained; [L] is the phospholipid concentration; K_P is the molecular lipid/water partition coefficient, and γ_L being the molar volume of the lipid (ca. 0.7 dm^3 mol^{-1}).[23,24] The spectral shifts relative to each system were obtained by the difference between the wavelengths in the presence and absence of LUVs. Then, these values were used to construct a graph of the spectral shift variation as a function of lipid concentration. All the spectra were obtained at room temperature and corrected for dilution effect (subtraction of respective baselines).

Turbidity measurements

Absorption spectra collected for the ε determination in the presence of LUVs were analyzed for their relative change in turbidity at 500 nm.[25-27] These changes were plotted as a function of the concentration of the antioxidant.[27]

Results and Discussion

In order to investigate the interaction of the antioxidants with model membranes representing both healthy and cancerous cells, three distinct experimental conditions were considered. The first condition mimics a healthy cellular environment, characterized by a neutral pH (ca. 7.4) and a membrane predominantly composed of phosphatidylcholine and cholesterol named PC/Chol. The aLUV, also representative of healthy cells, involves an asymmetric model membrane with phosphatidylcholine and cholesterol in the outer leaflet, and phosphatidylethanolamine and cholesterol in the inner leaflet, at a similar pH (ca. 7.4). The third condition models a cancerous cellular environment, where lipid asymmetry is lost, resulting in phosphatidylserine and phosphatidylethanolamine being present in the outer leaflet of the membrane. This condition also simulates the acidic microenvironment typical of cancer cells (pH ca. 5.5).[20] It is important to emphasize that, although a vast array of antioxidant compounds exists, QUE and TA were specifically chosen for this study due to their shared biological activities and their contrasting structural

characteristics, including molecular weight, size, and water solubility. These compounds were selected because they both exhibit antioxidant properties highly relevant to the context of cancer and cellular membrane interactions. By focusing on these two antioxidants, the study aimed to investigate how differences in structural attributes influence their behavior, particularly in the context of cancer-related alterations in cell membrane properties.

An initial investigation was conducted to assess the intrinsic spectrophotometric properties of the compounds and how these properties are influenced by the specific environments examined in this study. At this stage, the absorbance was obtained as a function of bioactive increasing concentrations in buffer (pHs 5.5 and 7.4) and in the presence of model membranes mimetic of cancer and healthy cells. Figures 2a-2b exemplifies the spectral behavior of each compound as a function of antioxidants concentrations. It is possible to notice that there is an increase in absorbance intensity with increasing concentration. The maximum absorbance remains at the same position throughout the range, with λ_{max} for quercetin and tannic acid positioned at 375 and 278 nm, respectively. The maximum absorbance at each concentration was used to construct the graphs in Figures 2c-2d, from which it was possible to determine the molar absorptivity coefficient (ε) of the antioxidants (Table 1). The pH variation had a slight influence on the ε values for polyphenolic compounds. TA showed higher ε values under acidic conditions, whereas QUE demonstrated

Table 1. Molar absorptivity coefficient (ε) of quercetin (QUE) and tannic acid (TA) in the presence and absence of model membranes of healthy (PC/Chol, aLUV) and cancer (PC/PE/PS/Chol) cells

	QUE ε / (L mol^{-1} cm^{-1})	TA ε / (L mol^{-1} cm^{-1})
Citrate phosphate buffer		
pH 5.5	0.0205 ± 0.0005	0.0139 ± 0.0004
pH 7.4	0.0189 ± 0.0001	0.0157 ± 0.0011
PC/PE/PS/Chol	0.0215 ± 0.0001	0.0197 ± 0.0014
PC/Chol	0.0198 ± 0.0003	0.0137 ± 0.0017
aLUV	0.0204 ± 0.0007	0.0156 ± 0.0015

PC: 1-palmitoyl-2-oleoyl-*sn*-glycero-3-phosphocholine; PE: 1-palmitoyl-2-oleoyl-*sn*-glycero-3-phosphatidylethanolamine; PS: 1-palmitoyl-2-oleoyl-*sn*-glycero-3-phosphatidylserine; Chol: cholesterol; aLUV: asymmetric large unilamellar vesicles.

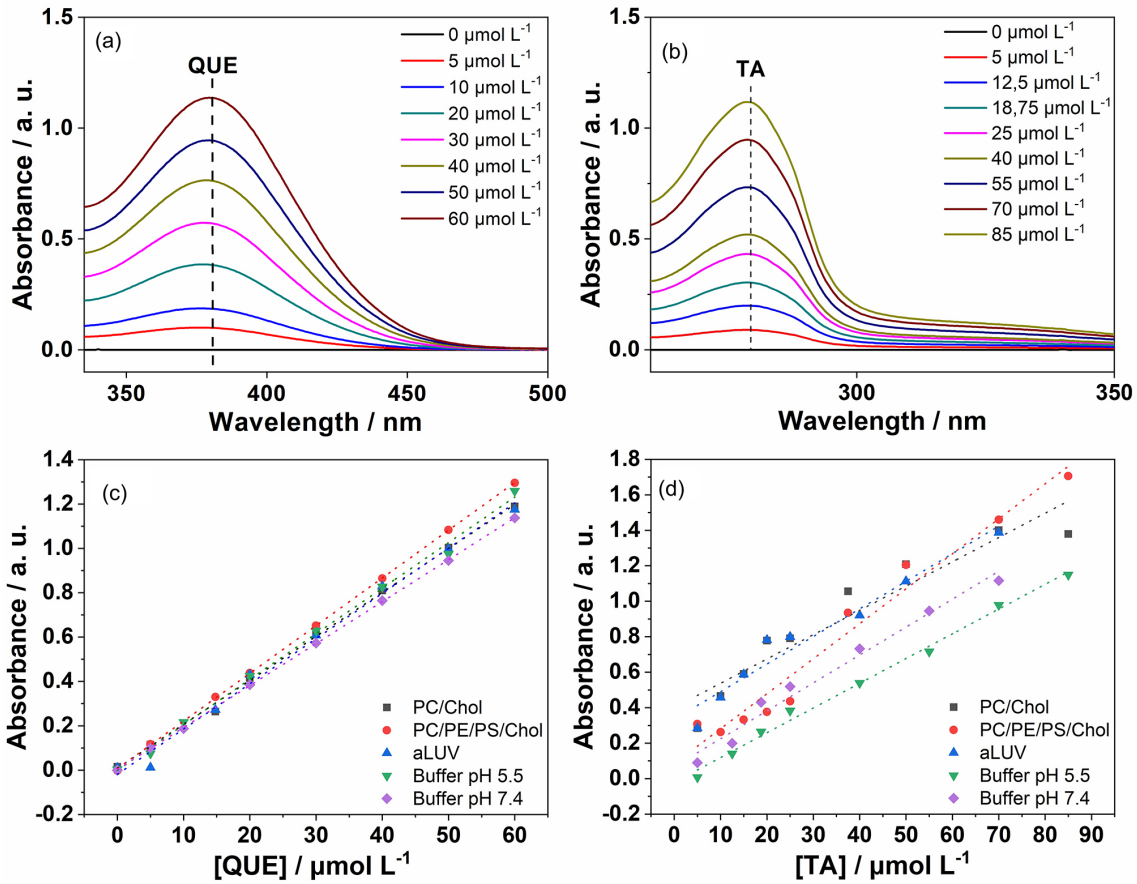

Figure 2. Spectral behavior as a function of increasing concentrations of antioxidants. (a) QUE in citrate phosphate buffer, pH 7.4; (b) TA in citrate phosphate buffer, pH 7.4. Maximum absorbance at each bioactive concentration used to determine molar absorptivity coefficients in the presence and absence of LUVs and aLUV: (c) QUE, and (d) TA. The dotted line was obtained by linear fit.

the opposite. In the presence of the model membranes, it was possible to notice a slight increase in this parameter for QUE when comparing the ε values obtained in the absence and in the presence of lipid. This behavior is considerably more pronounced for TA in the presence of cancer models. Given that an increase in ε can be associated with the interaction of bioactive compounds with environments of lower polarity,[28] these results suggest that both QUE and TA are likely interacting with the lipid systems.

The affinity of the compounds for cancer and healthy cell mimetic systems was explored by determining their partition coefficients under the aforementioned conditions. For that, solutions of the bioactive compounds were titrated with increasing concentration of LUVs or aLUVs. As result, all the polyphenolic compounds exhibited an increase in absorbance intensity after the addition of lipids, which was accompanied by spectral shifts from the maximum absorbance (see Figure 3a). Through the literature,[29-31] it is possible to notice that this behavior is common among polyphenolic compounds when they interact with lipid systems and reflects that these bioactives are migrating from a polar to a nonpolar environment. These findings indicate that QUE and TA are indeed interacting with the model membranes under study. In search of quantify this interaction, the bioactive absorbance at each lipid concentration was normalized and used to obtain the partition isotherms shown in Figures 3b and 3c. The resultant curve was nonlinear adjusted by equation 1 for the obtention of the partition coefficients, K_P (Table 2). The values obtained by QUE and TA for PC/Chol (80:20) are in good agreement with those found in literature at similar experimental conditions.[32,33] These results are also consistent with those obtained in the presence of aLUVs. Considering that the outer leaflet of this system presents the same lipid composition of PC/Chol LUVs, it indicates that the outer leaflet of the lipid bilayer plays a critical role in the partitioning of these bioactives into healthy cell-mimetic membranes.

Despite the similarities in spectral changes with increasing lipid concentration, QUE and TA exhibited distinct behaviors depending on the lipid composition.

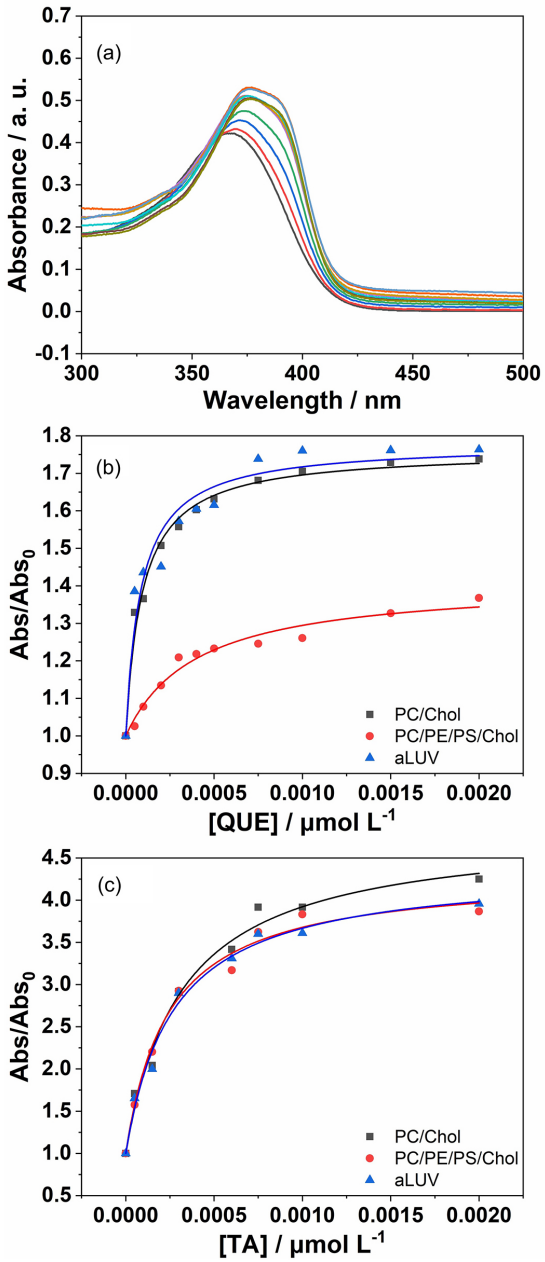

Figure 3. (a) Representative spectrum QUE in PC/PE/PS/Chol LUV (0-2000 μmol L^{-1}), (b) QUE and (c) TA K_P determination values in the presence of LUVs and aLUV (100 μmol L^{-1}), pH 7.4 (PC/Chol and aLUV) and pH 5.5 (PC/PE/PS/Chol). Continuous line was obtained using the nonlinear fit shown in equation 1. The experiments were performed at 25 ± 2 °C.

Table 2. Partition coefficients (K_P), maximum spectral shift ($\Delta\lambda_{max}$) and free energy of partition (ΔG_P), $\Delta G_P = -RT\ln 55.5K_P$, (R is the universal gas constant and T is the temperature)[34] of quercetin (QUE) and tannic acid (TA) in model membranes of healthy (PC/Chol, aLUV) and cancer (PC/PE/PS/Chol) cells

Phenol	PC/PE/PS/Chol			PC/Chol			aLUV		
	K_P / (L mol^{-1})	$\Delta\lambda_{max}$ / nm	ΔG_P / (kcal mol^{-1})	K_P / (L mol^{-1})	$\Delta\lambda_{max}$ / nm	ΔG_P / (kcal mol^{-1})	K_P / (L mol^{-1})	$\Delta\lambda_{max}$ / nm	ΔG_P / (kcal mol^{-1})
QUE	3400 ± 600	11	−7.25	14700 ± 1600	6	−8.13	15800 ± 3600	9	−8.17
TA	5700 ± 800	7	−7.56	4400 ± 700	2.5	−7.40	5100 ± 700	2	−7.49

PC: 1-palmitoyl-2-oleoyl-*sn*-glycero-3-phosphocholine; PE: 1-palmitoyl- 2-oleoyl-*sn*-glycero-3-phosphatidylethanolamine; PS: 1-palmitoyl- 2-oleoyl-*sn*-glycero-3-phosphatidylserine; Chol: cholesterol; aLUV: asymmetric large unilamellar vesicles.

QUE demonstrated greater partitioning into the healthy cell models, consistent with its high affinity for cholesterol as reported in previous studies.[35] However, the presence of PE and PS significantly reduced its partitioning. This behavior may be associated with the anionic character presented by both QUE and PC/PE/PS/Chol membranes.[14] Added to this, the number of possibilities for carrying out hydrogen bonds between QUE and the membrane is reduced at pH 5.5 due to the degree of protonation of the species involved. TA partitions slightly more to the mimetic membranes of cancer cells than to healthy ones. Unlike QUE, it is a hydrophilic compound, which means that the interaction associated with quercetin's hydrophobicity, possibly responsible for potentiating its partition into PC/Chol and aLUV, is not present in the TA-membrane interaction. In spite of this, the order of magnitude obtained for the K_p provides evidence that the TA-membrane interaction also involves a balance between non-electrostatic and electrostatic components.[33] Thus, the electrostatic repulsion due to the anionic character of TA and PC/PE/PS/Chol membranes did not affect its partition, an indication that this effect is driven by non-electrostatic interactions. Thus, it is possible that the TA-membrane interaction is driven especially by non-electrostatic interactions. Indeed, Kalina and Pease[36] demonstrated that TA exhibits less interaction with PS lipids than PC due to the specificity of TA for the choline group of PC. However, our results indicate that this specificity is not effective to ensure greater TA partitioning for PC/Chol and aLUV membranes in comparison to PC/PE/PS/Chol. However, it may be contributing to the pronounced interaction in the cancer mimetic environment, which contains PC and PS in similar concentrations.

These findings suggest that the two polyphenols interact differently with the studied lipid membranes, which is possibly associated with their hydrophobicity/hydrophilicity. The hydrophilic TA is influenced by the lipid composition of cancer cells to the point of having a greater affinity for them. The hydrophobic QUE is also influenced by the lipid composition of these cells; however, this interaction indicates that the cellular changes triggered by cancer do not contribute to increase their affinity for these cell membranes. By analyzing the differences between these molecules, it is possible to identify that the number of groups available for carrying out hydrogen bonds between the polyphenol and the membrane can be a relevant factor in the interaction. TA and QUE are influenced by the acidic pH variation that protonates many of the groups available for this type of interaction. However, TA still has a significant number of available groups (about eight hydroxyls), unlike QUE (at most one hydroxyl) as can be seen in Figure 1.

The partition free energies of QUE and TA were evaluated (see Table 2) in order to estimate their order of magnitude and how they relate to their hydrophobicity/hydrophilicity differences. It is possible to notice that for the hydrophobic compound (QUE) the partition free energy in PC/Chol is smaller than that obtained for the hydrophilic one (TA). This indicates that the partition of the hydrophobic compound for neutral membranes is energetically more favorable than the hydrophilic one in line with Iyer *et al*.,[37] Monroe *et al*.[38] and Galassi *et al*.[39] However, when considering the anionic character membrane, it is noted that the partitioning is equally favorable for both compounds, evidencing the presence of a balance between electrostatic and non-electrostatic contributions in the interaction of these compounds with the model membranes.

Spectral shifts were also used to explore the interaction of antioxidants with lipid systems. Figure 4 shows the changes of this parameter as a function of the lipid concentration. The total variations are shown in Table 2. For both compounds, the intrinsic absorbance was used as a strategy to study the antioxidant-membrane interaction. The spectral shift is able to reflect variations in the microenvironment of these compounds. The greater the displacement, the more nonpolar the medium in which the compound is found.[40-42] It is possible to notice that the data obtained for TA reflects that it can assume a superficial location, near the polar heads, in both lipid compositions. This is in agreement with the data from Andrade *et al*.[33] by fluorescence quenching. QUE also exhibits a superficial location in PC/Chol and aLUV membranes, which is also in agreement with the literature.[33] The superficial localization of QUE in healthy model membranes is further supported by the spectral shift observed in the presence of aLUVs, which remained unaffected by the presence of the membrane-fluidizing lipid, PE.[43] However, the most pronounced spectral shift occurs for QUE in the presence of both PE and PS. This can be attributed to the ability of PE to fluidize the outer leaflet of the membrane, allowing the phenol groups of QUE to be accommodated in a more nonpolar region than the membrane/buffer interface.[43]

Turbidity tests were performed by monitoring the absorbance at 500 nm of 100 μmol L^{-1} of LUVs or aLUVs under increasing concentration of the bioactives, as shown in Figure 5. These results show that QUE induces an increase in turbidity in the systems that mimics healthy cells (Figure 5a), indicating that in addition to having a high affinity for this system, (Table 2) the bioactive promotes the aggregation of vesicles. In contrast, QUE does not significantly vary the turbidity of the system that mimics cancer cells. TA, on the other hand, induces an increase

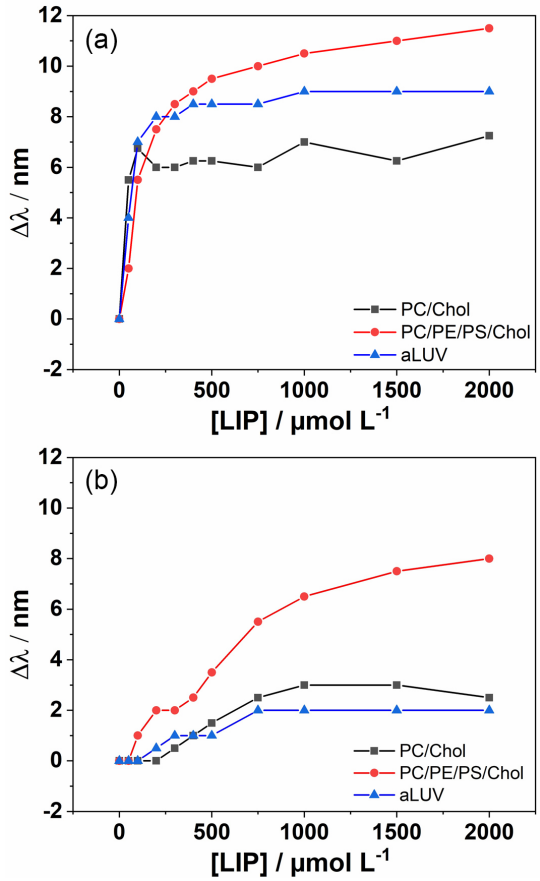

Figure 4. (a) QUE and (b) TA spectral shift under increasing lipid concentrations (0-2000 μmol L^{-1}). Solid lines are used as guide.

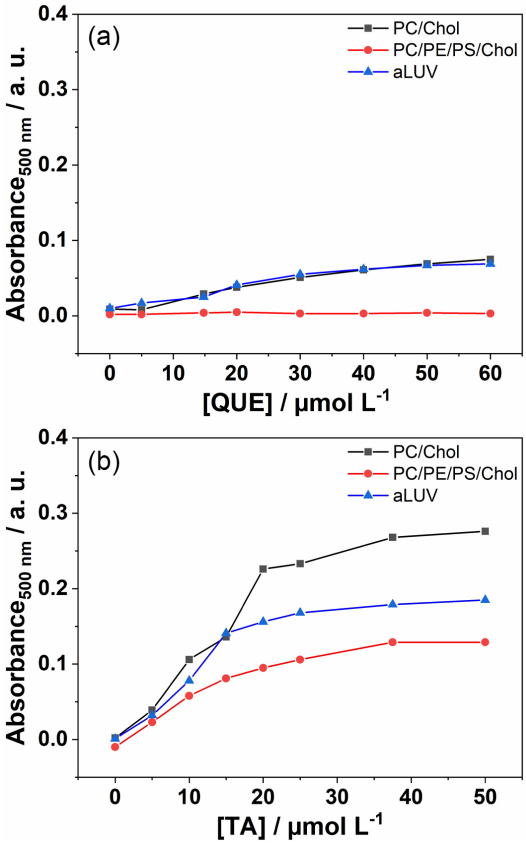

Figure 5. Detergent action of (a) QUE and (b) TA on lipid membranes PC/PE/PS/Chol, at pH 5.5 and PC/Chol and aLUV, at pH 7.4. Solid lines are used as guide.

in the intensity of absorbance in both healthy and cancer models (Figure 5b). This result is an indication that TA promotes an aggregation effect of model membranes as observed by Simon *et al.*[44] and Leite *et al.*[27] For the mimetic membranes of healthy cells, it is possible to notice a greater tendency of aggregation in relation to those that mimic the cancer ones. This result may be associated with the electrical charge properties of the bioactive and the lipid systems, since the reduction of the aggregation effect occurs for the system in which both membrane and bioactive have an anionic character, in which electrostatic repulsion can contribute to the reduction of aggregation.[14] In contrast, this electrostatic repulsion must be minimized in healthy cell mimetics because the membranes are zwitterionic.

Simon *et al.*[44] described that the aggregation tendency of zwitterionic liposomes induced by TA can be attributed to the formation of multiple hydrogen bonds and this can be related to the charge properties of the bioactive at different pHs.[14] At pH 7.4, there is a greater amount of deprotonated hydroxyl groups than at pH 5.5 and, therefore, a greater tendency to form multiple hydrogen bonds and, consequently, a greater tendency to aggregation. Furthermore, this result contributes to the understanding of the difference in TA partitioning by the mimetic systems of healthy and cancer cells. Thus, the aggregation tendency may be the factor responsible for impairing the partitioning of TA by electrically neutral membranes, as the highest aggregation tendency was observed for the system that exhibited the lowest partition coefficient. The same does not apply to QUE, where the greatest partitioning occurs in the composition in which the aggregation is observed. This difference can be related to differences in the hydrophobicity/hydrophilicity of these antioxidants and their location on the membrane. As previously discussed, the hydrophilic TA may prefer to be located in more superficial regions than the hydrophobic QUE. Consequently, the aggregation effect induced by antioxidants should be minimized when they are located deeper in membrane, as well as when they present a small size and has few groups available for hydrogen bonding. However, it is still important to point out that the conditions under which QUE and TA exhibit the greatest partitioning in the model membranes correspond to a similar pattern of aggregation (Figures 5a and 5b) and similar spectral shifts (Table 2), suggesting that the balance between electrostatic and non-electrostatic interactions in the system seems to be

essential for TA and QUE to be able to differentiate healthy cell membranes from cancerous ones.

The results of this study underscore the relevance of membrane biophysics approaches in elucidating the impact of cell membrane microenvironment variations on interactions with distinct biomolecules. Although based on simplified cell models, this research provides valuable insights into the activity of the studied antioxidants, QUE and TA. Furthermore, it establishes a foundation for future investigations employing more biologically complex strategies, including *in vitro* and *in vivo* analyses, as well as their integration with established chemotherapeutic agents. Such studies may provide deeper insights into the detailed mechanistic pathways underlying the activity of these antioxidants, advancing both fundamental knowledge and their potential therapeutic applications. Finally, the findings of this work represent a step forward in bridging fundamental biophysical research and potential therapeutic applications.

Conclusions

We explored the interaction of two antioxidants with membrane mimetic models of healthy and cancer cells. Although these compounds have properties against different types and cancer, there is still no clarity about the mechanism by which they act. In this sense, this work could contribute to gather elements that help in the understanding of their activities. Our results showed that QUE and TA interact differently with distinct model membranes. QUE has greater affinity for the mimetic membranes of healthy cells while TA has it for cancer ones. These findings are attributed to the existence of a balance between electrostatic and non-electrostatic interactions in the system, which is dependent of the polyphenols hydrophobicity/hydrophilicity and number of groups available for hydrogen bonding. In addition, it was possible to conclude that the lipid membrane, its composition and the pH of the cellular microenvironment are capable of affecting the interaction of these antioxidants with the target organisms. This work paves the way for new possibilities, highlighting the need for a systematic investigation into the contribution of individual lipids. Additionally, incorporating other experimental approaches would be valuable in further clarifying the specific role of each element within this system.

Acknowledgments

N. B. L. Slade would like to acknowledge the financial support received from the Research Supporting Foundation of Minas Gerais State (FAPEMIG-Brazil) (grant APQ-0554-21) and National Council for Scientific and Technological Development (grant 405457/2023-5). J. A. Moreto is grateful for the financial support received from the National Council for Scientific and Technological Development (CNPq-Brazil) (process: 303659/2019-0) and the Minas Gerais State Agency for Research and Development (FAPEMIG-Brazil) (process: APQ-02276-18). The authors are also thankful to the Rede Mineira de Materiais Inorgânicos (RM²I), a research group supported by FAPEMIG (RED-00116-23). Oliveira and Mendes also thank the Coordination for the Improvement of Higher Education Personnel (CAPES) for the scholarship and Programa de Pós-graduação em Ciência e Tecnologia de Materiais (PPGCTM - UFTM).

Author Contributions

Pablo A. Oliveira was responsible for investigation, formal analysis and writing-up; Leandro A. Mendes for investigation, formal analysis and writing-up; Vitor O. Silva for investigation; Paulo V. Scarparo for investigation; Layra C. Conceição for investigation; Pedro I. S. Maia for formal analysis; Jéferson A. Moreto for formal analysis; Natália B. Leite Slade for supervision, project administration, writing-up, and formal analysis.

References

1. Badrloo, M. A.; Pourmadadi, M.; Abdouss, M.; Rahdar, A.; Pandey, S.; Fathi-Karkan, S.; *Ind. Crops Prod.* **2024**, *218*, 118939. [Crossref]
2. Arif, A.; Khar, M. S.; Shahid, N.; Aman, W.; Javed, J.; Rubab, A.; Nayab, M.; Mastoor, K.; Arshad, R.; Rahdar, A.; Fathi-karkan, S.; Kharaba, Z.; Pandey, S.; *Eur. J. Med. Chem. Rep*. **2024**, *12*, 100219. [Crossref]
3. Hosseini, Z. S.; Zeinalilathori, S.; Fathi-karkan, S.; Zeinali, S.; Rahdar, A.; Siddiqui, B.; Kharaba, Z.; Pandey, S.; *J. Drug Delivery Sci. Technol.* **2024**, *101*, 106220. [Crossref]
4. Holghoomi, R.; Kharab, Z.; Rahdar, A.; Pandey, S.; Ferreira, L. F. R.; *Coord. Chem. Rev.* **2024**, *513*, 215903. [Crossref]
5. Najafi, M.; Pourmadadi, M.; Abdous, M.; Rahdar, A.; Pandey, S.; *J. Mol. Liq.* **2024**, *400*, 124543. [Crossref]
6. Li, S.; Chen, G.; Zhang, C.; Wu, M.; Wu, S.; *Food Sci. Hum. Wellness* **2014**, *3*, 110. [Crossref]
7. Rauf, A.; Imran, M.; Khan, I. A.; Ur-Rehman, M.; Gilani, A. S.; *Phytother. Res.* **2018**, *32*, 2109. [Crossref]
8. Batiha, G. E. S.; Beshbishy, A. M.; Mulla, Z. S.; Ikram, M.; El-Hack, M. E. A.; Taha, A. E.; *Foods* **2020**, *3*, 374. [Crossref]
9. Jordan, L.; Booth, B. W.; *J. Biomed. Mater. Res. A* **2017**, *106*, 26. [Crossref]

10. Baldwin, A.; Booth, B. W.; *J. Biomater. Appl.* **2022**, *36*, 1. [Crossref]
11. Kaczmarek, B.; *Materials* **2020**, *13*, 3224. [Crossref]
12. Baer-Dubowska, W.; Szaefer, H.; Celińska, A.; Kuzniak, V.; *Curr. Pharmacol. Rep.* **2020**, *6*, 28. [Crossref]
13. Sundaram, M. K.; Raina, R.; Afroze, N.; Bajbouj, K.; Hamad, M.; Haque, S.; Hussain, A.; *Biosci. Rep*. **2019**, *39*, BSR20190720. [Crossref]
14. Mendes, L. A.; Farnesi-de-Assunção, T. S.; Oliveira, P. A.; Rotta, I. S.; Moreto, J. A.; Devienne, K. F.; Paiva, A. D.; Slade, N. B. L.; *Nano Trends* **2024**, *7*, 100040. [Crossref]
15. Custódio, L.; Mendes, L. A.; Alvares, D. S.; Moreto, J. A.; Slade, N. B. L.; *Bull. Mater. Sci.* **2022**, *45*, 159. [Crossref]
16. Heidari, F.; Akbarzadeh, I.; Nourouzian, D.; Mirzaie, A.; Bakhshandeh, H.; *Adv. Powder Technol.* **2020**, *31*, 4768. [Crossref]
17. Keshavarz, F.; Dorfaki, M.; Bardania, H.; Khosravani, F.; Nazari, P.; Ghalamfarsa, G.; *Iran. J. Basic. Med. Sci.* **2023**, *48*, 321. [Crossref]
18. Chimento, A.; De Luca, A.; D'Amico, M.; De Amicis, F.; Pezzi, V.; *Int. J. Mol. Sci*. **2023**, *24*, 1680. [Crossref]
19. Lizenko, M. V.; Regerand, T. I.; Bakhirev, A. M.; Lizenko, E. I.; *J. Evol. Biochem. Phys.* **2011**, *47*, 428. [Crossref]
20. Dhup, S.; Dadhich, K.; Porporato, P.; Sonveaux, P.; *Curr. Pharm. Des.* **2012**, *18*, 1319. [Crossref]
21. Tan, L.; Chan, K.; Pusparajah, P.; Lee, W. L.; Chuah, L.; Khan, T.; Lee, L. H.; Goh, B. H.; *Front. Pharmacol.* **2017**, *8*, 12. [Crossref]
22. Doktorova, M.; Heberle, F. A.; Eicher, B.; Standaert, R. F.; Katsaras, J.; London, E.; Pabst, G.; Marquardt, D.; *Nat. Protoc.* **2018**, *13*, 2086. [Crossref]
23. Santos, N. C.; Prieto, M.; Castanho, M. A.; *Biochim. Biophys. Acta, Biomembr*. **2003**, *1612*, 123. [Crossref]
24. Marsh, D.; *Chem. Phys. Lipids* **2010**, *163*, 667. [Crossref]
25. Mattei, B.; França, A. D. C.; Riske, K. A.; *Langmuir* **2015**, *31*, 378. [Crossref]
26. Ahyayauch, H.; Collado, I. M.; Alonso, A.; Goñi, F. M.; *Biophys. J.* **2012**, *102*, 2510. [Crossref]
27. Leite, N. B.; Martins, D. B.; Fazani, V. E.; Vieira, M. R.; dos Santos, M. P.; *Biochim. Biophys. Acta, Biomembr.* **2018**, *1860*, 2320. [Crossref]
28. Wang, Z.; Leung, M. H.; Kee, T. W.; English, D. S.; *Langmuir* **2010**, *26*, 5520. [Crossref]
29. Costa, M.; Losada-Barreiro, S.; Paiva-Martins, F.; Bravo-Díaz, C.; *Foods* **2021**, *10*, 539. [Crossref]
30. Brglez Mojzer, E.; Knez Hrnčič, M.; Škerget, M.; Knez, Ž.; Bren, U.; *Molecules* **2016**, *7*, 901. [Crossref]
31. Yu, X.; Chu, S.; Hagerman, A. E.; Lorigan, G. A.; *Food Chem.* **2011**, *59*, 6783. [Crossref]
32. Leite, N. B.; Martins, D. B.; Alvares, D. S.; Cabrera, M. P. S.; *Chem. Phys. Lipids* **2021**, *242*, 105. [Crossref]
33. Andrade, S.; Ramalho, M. J.; Loureiro, J. Á.; Pereira, M. C.; *Colloids Surf., B* **2019**, *180*, 83. [Crossref]
34. Leite, N. B.; dos Santos Alvares, D.; de Souza, B. M.; Palma, M. S.; Ruggiero Neto, J.; *Eur. Biophys. J.* **2014**, *43*, 121. [Crossref]
35. De Granada-Flor, C.; Sousa, H. A. L.; Filipe, M.; Santos, R. F. M.; de Almeida, L.; *Chem. Commun.* **2019**, *55*, 1750. [Crossref]
36. Kalina, M.; Pease, D. C.; *J. Cell Biol.* **1977**, *74*, 726. [Crossref]
37. Iyer, B. R.; Mahalakshmi, R.; *Biophys. J.* **2019**, *117*, 25. [Crossref]
38. Monroe, J. I.; Shell, M. S.; *Proc. Natl. Acad. Sci*. **2018**, *115*, 8093. [Crossref]
39. Galassi, V. V.; Arantes, G. M.; *Biochim. Biophys. Acta, Bioenerg.* **2015**, *1847*, 1560. [Crossref]
40. Vilková, M.; Hudáčová, M.; Palušeková, N.; Jendželovský, R.; Almáši, M.; Béres, T.; Fedoročko, P.; Kožurková, M.; *Molecules* **2022**, *27*, 2883. [Crossref]
41. Kamaly, N.; Yameen, B.; Wu, J.; Farokhzad, O. C.; *Chem. Rev.* **2016**, *116*, 2602. [Crossref]
42. Dahiya, P.; Choudhury, S. D.; Maity, D. K.; Mukherjee, T.; Pal, H.; *Spectrochim. Acta, Part A* **2008**, *69*, 134. [Crossref]
43. Dawaliby, R.; Trubbia, C.; Delporte, C.; Noyon, C.; Ruysschaert, J. M.; Van Antwerpen, P.; Govaerts, C.; *J. Biol. Chem.* **2016**, *291*, 3658. [Crossref]
44. Simon, S.; Disalvo, E.; Gawrisch, K.; Borovyagin, V.; Toone, E.; Schiffman, S.; Needham, D.; Mcintosh, T.; *Biophys. J.* **1994**, *66*, 1943. [Crossref]

Submitted: September 27, 2024
Published online: January 20, 2025